ENERGETIC AND ENTROPY ANALYSIS OF A NOVEL TRANSCRITICAL CO_2 TWO-STAGE COMPRESSION/EJECTOR REFRIGERATION CYCLE FOR SHIPBOARD COLD CHAMBER

by

Dazhang YANG[a,b,c,d], Yang LI[a,b,c,d], Jing XIE[a,b,c,d,*], and Jinfeng WANG[a,b,c,d]

[a] College of Food Science and Technology, Shanghai Ocean University, Shanghai, China
[b] Professional Technology Service Platform on Cold Chain Equipment Performance and Energy Saving Evaluation, Shanghai, China
[c] Experimental Teaching Demonstration Center for Food Science and Engineering, Shanghai Ocean University, Shanghai, China
[d] Inspection and Testing Center for Cold Storage and Refrigeration Equipment, Ministry of Agriculture, Quality Supervision, Shanghai, China

Original scientific paper
https://doi.org/10.2298/TSCI220702181Y

The adverse effects of global warming and climate change require critical measures for marine refrigeration technology because of its impact on GHG emissions. A novel transcritical CO_2 two-stage compression/ejector refrigeration cycle for shipboard cold chamber is proposed in this research. A comparative analysis was conducted between the basic transcritical CO_2 two-stage compression cycle and the cycle equipped with a two-phase ejector considering the COP. Meanwhile, the refrigeration cycle was analyzed using entropy analysis to elucidate the distribution of irreversible losses in each component of the two-stage compression/ejector refrigeration cycle, and the effects of system parameters such as the evaporating and gas cooler outlet temperatures as well as the intermediate and discharge pressures on the cycle were investigated. The results showed that the ejector had the largest power capability loss, accounting for 26.95 % of the overall system, which is followed by the low pressure compressor with 26.06%. The COP of basic and ejector system significantly increase as the gas cooler outlet temperature and intermediate pressure decrease as well as the evaporating temperature increases. Furthermore, the entropy production of the system components decreases gradually with increasing evaporating temperature, with the greatest reduction in the ejector. In addition, the entropy production of the two-phase ejector remains constant with the increase of the high pressure side discharge pressure and gas cooler outlet temperature.

Key words*: energetic analysis, entropy analysis, COP, transcritical CO_2 refrigeration cycle, two-phase ejector*

Introduction

With the increasing awareness of environmental protection, climate issues are receiving more and more attention. The shipping industry accounts for more than 80% of the global trade traffic and makes a tremendous contribution the world economy [1]. But on the other hand, such a large volume of transportation leads to serious air pollution in regard to the ship's

* Corresponding author, e-mail: jxie@shou.edu.cn

exhaust gases. The shipboard cold chamber can be used to store food to meet the living demand of the ship's staff, which is one of the high energy-consuming equipment of modern ships [2]. Therefore, the ship's energy saving and emission reduction is urgent.

Based on the greenhouse effect and ozone layer depletion, traditional CFC refrigerants are being phased out, while HCFC and HFC refrigerants are also being restricted. Natural refrigerants are increasingly favored in the refrigeration field. The CO_2 has made a big impact in the refrigeration field with its excellent performance as a natural refrigerant. It has excellent environmental performance: its global warming potential (GWP) is one, its ozone depletion potential (ODP) is zero, it has a large latent heat of vaporization, it is non-toxic, it has non-spontaneous combustion and is of low cost [3, 4]. Besides, the critical temperature of CO_2 is 31.1 ℃ and the critical pressure is 7.38 MPa. Due to this thermodynamic characteristic, most of the refrigeration systems using CO_2 operate in the transcritical region. We know that the basic transcritical CO_2 refrigeration system brings a large throttling loss, so the measure of using ejectors to recover energy is getting more and more attention from the researchers [5]. In addition, the energy analysis method on the basis of the First law of thermodynamics, which considers the COP of the refrigeration cycle as an evaluation index, cannot make an assessment of energy loss and transfer direction. On the other hand, entropy analysis can make a more comprehensive analysis of the energy utilization of the system [6].

Farzaneh *et al.* [7] studied the ejector and found that increasing the length and diameter of the equal-area cross-section and reducing the diameter of the working nozzle throat resulted in a 32% increase in the entrainment ratio and COP, and a decrease in total entropy production. Ji *et al.* [8] analyzed the solar ejector refrigeration cycle using entropy analysis and found that the collector and ejector accounted for the largest irreversible losses. In addition, for a certain evaporating temperature, there is an optimum temperature at which the irreversible losses of the whole solar ejector refrigeration cycle are minimized and the performance is optimal, while the other operating parameters of the system remain unchanged. Ramirez-Minguela *et al.* [9] performed an entropy generation analysis of a solid oxide fuel cell and found significant differences in local and global entropy generation in different cases. A two-stage CO_2 transcritical mechanical compression cooling cycle with an ejector was investigated by Volodymyr *et al.* [10]. It was found that compared with the conventional system, the efficiency of the two-stage CO_2 transcritical mechanical compression chiller is increased by 32.7% in transcritical operating conditions at high ambient temperatures. Zeng *et al.* [11] used a multi-parameter optimization approach to thermodynamically analysis the dual-ejector cycle and compared it with a conventional two-stage transcritical CO_2 refrigeration cycle. It was found that the COP of the transcritical CO_2 refrigeration cycle with double ejectors is on average about 42% higher than that of the conventional cycle.

This paper proposes a novel transcritical CO_2 two-stage compression/ejector refrigeration cycle for shipboard cold chamber with an ejector placed between the low pressure compressor and high pressure compressor in an attempt to increase the suction pressure of the low pressure compressor and further improve the system performance. In this paper, the transcritical CO_2 two-stage compression refrigeration system with an ejector is studied theoretically using energy analysis and entropy analysis, and compared with the basic transcritical CO_2 two-stage compression refrigeration system. The entropy production distribution of each component in the compression/ejector two-stage refrigeration system and the effects of gas cooler outlet temperature, evaporating temperature, intermediate and discharge pressures on the system COP and component entropy production were also investigated. The purpose of this research is to propose a novel two-stage transcritical CO_2 cycle equipped with a two-phase ejector for ship-

board cold chamber and also to provide some guidance for energy saving and emission reduction of marine refrigeration systems.

System description and modelling

System description

Figure 1(a) depicts the schematic diagram of a conventional transcritical CO_2 two-stage compression refrigeration cycle (CTRC), and the corresponding pressure-enthalpy diagram of the CTRC system is presented in fig. 1(b). As illustrated in fig. 1(a), the CTRC system consists of seven components, including a gas cooler, a high pressure expansion valve (HP EV), an intercooler (or a simple mixer/phase separator), a high pressure (HP) compressor, a low pressure (LP) compressor, a low pressure expansion valve (LP EV) and an evaporator. The working principle of the CTRC system is as: Saturated vapor from the outlet of the evaporator (state Point 1) is compressed by a LP compressor into superheated vapor (state Point 2), which then passes into the intercooler. Saturated vapor from the outlet of the intercooler (state Point 3) is compressed into HP and high temperature vapor (state Point 4) by a HP compressor, and then passes through the gas cooler for constant pressure cooling. The supercritical fluid from the outlet of the gas cooler (state Point 5) is depressurized through a HP EV (state Point 6) and then enters the intercooler. In addition, the saturated fluid from the outlet of the intercooler (state Point 7) passes through the LP EV for depressurization (state Point 8) and enters the evaporator.

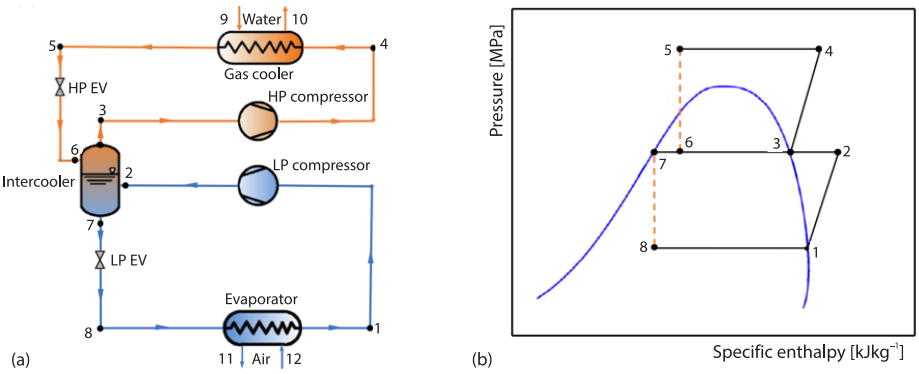

Figure 1. The schematic diagram for the CTRC system (a) and the corresponding pressure-enthalpy diagram (b)

Figure 2(a) exhibits the schematic diagram of a novel transcritical CO_2 two-stage compression/ejector refrigeration cycle (TERC) for shipboard cold chamber, and fig. 2(b) demonstrates the corresponding pressure-enthalpy diagram of the TERC system. As shown in fig. 2(a), the TERC system is composed of a gas cooler, a HP EV, an intercooler (or a simple mixer/phase separator), a HP compressor, a LP compressor, a LP EV, a two-phase ejector, an evaporator and a gas-liquid separator. The TERC system works as: The saturated vapor (state Point 3) from the intercooler outlet is split into two portions. One portion of the fluid is compressed into HP and high temperature vapor (state point 4), and then circulates through the gas cooler for constant pressure cooling. The supercritical fluid-flowing from the gas cooler (state Point 5) is depressurized through the HP EV (state Point 6) and enters the intercooler. Another portion of the fluid enters the two-phase ejector as the primary flow (process 3-11) to entrain the saturated vapor from the evaporator (process 9 and 10). These two fluids are mixed and pressurized through the two-phase ejector (process 11-13), and then enters the gas-liquid separator.

The saturated vapor (state Point 1) from the gas-liquid separator outlet is compressed into medium pressure and temperature vapor (state Point 2) and then enters the intercooler. In addition, the saturated liquid (state Point 7) from the intercooler outlet is depressurized through the LP EV (state Point 8) and enters the evaporator. The performance of the TERC system is simulated using a thermodynamic analysis method, while the entropy production of the TERC system and its components is calculated. Meanwhile, the performance of the TERC system was compared with that of the CTRC system. The model proposed in this work is based on conservations of mass, momentum and energy. In addition, a 1-D isobaric mixing model is used for the performance analysis of the two-phase ejector. To simplify the thermodynamic analysis model, we made the following assumptions for the CTRC and TERC systems:

– The CTRC and TERC systems are assumed to operate under steady-state conditions [12].
– The flow in the two-phase ejector is treated by a 1-D flow model [13].
– The throttling processes of the HP and LP EV are isenthalpic.
– The compression process in both HP and LP compressor is an adiabatic and irreversible one.
– The pressure drop and heat loss of the refrigerant in the pipe-line are neglected [14].
– The working fluids leaving the evaporator, intercooler and gas-liquid separator are saturated.
– The kinetic energy at the inlet and outlet of the two-phase ejector is negligible [15].
– Generally, the isentropic efficiency of the working nozzle, mixing chamber and diffuser of the two-phase ejector is constant [16].

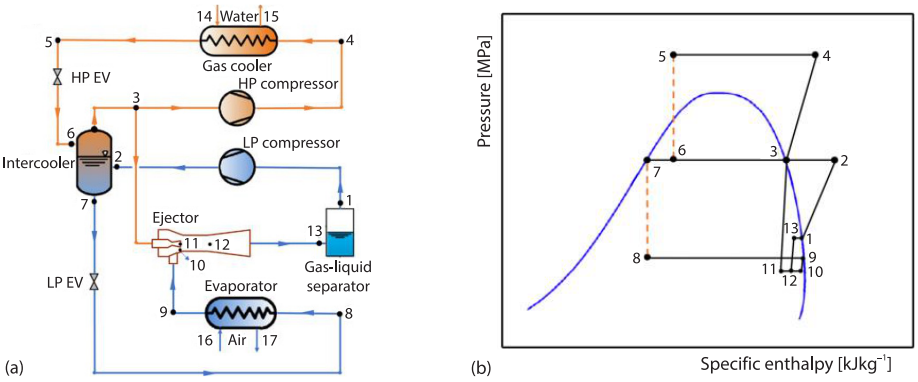

Figure 2. The schematic diagram for the TERC system (a) and the corresponding pressure-enthalpy diagram (b)

Two-phase ejector model

The ejector mainly consists of four parts, which are the working nozzle, the receiving chamber, the mixing chamber and the diffuser. Generally, the entrainment ratio, μ, can be used to asses performance of the two-phase ejector in terms of the TERC system [17].

The μ demonstrates the ability of the primary fluid to entrain the secondary fluid:

$$\mu = \frac{\dot{m}_9}{\dot{m}_{11}} = \sqrt{\eta_n \eta_m \eta_d \frac{h_{n,in} - h_{n,out,is}}{h_{d,out,is} - h_{m,out}}} - 1 \tag{1}$$

where parameters $\dot{m}_9$ and $\dot{m}_{11}$ are the mass-flow rates of the secondary and primary fluid of the two-phase ejector, respectively, η_n, η_m, and η_d – the efficiency of the working nozzle, mixing chamber and diffuser, $h_{n,in}$ and $h_{m,out}$ – the refrigerant specific enthalpy at the inlet of the working

nozzle and at the outlet of the mixing chamber, respectively, and $h_{n,out,is}$ and $h_{d,out,is}$ – the ideal outlet specific enthalpy at the working nozzle and diffuser after an isentropic process, respectively [18].

According to the principle of conservation of energy, ignoring the kinetic energy at the inlet of the two-phase ejector, the energy balance at the working nozzle can be expressed:

$$h_3 = h_{11} + \frac{1}{2}u_{11}^2 \tag{2}$$

where h_3 and h_{11} are the specific enthalpy of the primary flow entering and leaving the working nozzle, respectively.

The isentropic efficiency of the working nozzle η_n:

$$\eta_n = \frac{h_3 - h_{11}}{h_3 - h_{11s}} \tag{3}$$

where h_{11s} stands for the ideal exiting specific enthalpy through an isentropic expansion process in the working nozzle.

Since the kinetic energy of the secondary flow at the inlet of the suction chamber of the two-phase ejector is neglected, the energy balance of the suction chamber can be expressed:

$$h_9 = h_{10} + \frac{1}{2}u_{10}^2 \tag{4}$$

where h_9 and h_{10}, are the specific enthalpy of the secondary flow entering and leaving the working nozzle, respectively.

The isentropic efficiency of the suction chamber η_s can be expressed:

$$\eta_s = \frac{h_9 - h_{10}}{h_9 - h_{10s}} \tag{5}$$

where h_{10s} is the ideal exiting specific enthalpy through an isentropic expansion process in the suction chamber.

The steady-state steady flow energy equation can be expressed by eq. (6) in the mixing section:

$$\mu h_{10} + h_{11} + \frac{1}{2}\mu u_{10}^2 + \frac{1}{2}u_{11}^2 = (1+\mu)\left(\frac{1}{2}u_{12}^2 + h_{12}\right) \tag{6}$$

where the secondary flow velocity u_{10} is the negligible compared with the primary flow velocity u_{11}, so eq. (6) can be simplified:

$$\mu h_{10} + h_{11} + \frac{1}{2}u_{11}^2 = (1+\mu)\left(\frac{1}{2}u_{12}^2 + h_{12}\right) \tag{7}$$

The energy dissipation during the mixing process in the mixing chamber is consider in this research, so the mixing velocity:

$$u_{12} = \frac{u_{11}}{1+\mu}\sqrt{\eta_m} \tag{8}$$

Based on the principle of conservation of energy, the specific enthalpy of the mixed flow leaving the diffuser can be expressed:

$$h_{13} = h_{12} + \frac{1}{2}u_{12}^2 \tag{9}$$

where h_{12} and h_{13} are the specific enthalpy of the mixing flow entering and leaving the diffuser, respectively.

The isentropic efficiency of the diffuser η_d can be expressed:

$$\eta_d = \frac{h_{13s} - h_{12}}{h_{13} - h_{12}} \tag{10}$$

where h_{13s} is the ideal exit specific enthalpy for an isentropic expansion process within a diffusion process.

It is important to note that since the steady-state operation of the TERC system is bounded by mass conservation, the quality of the mixing flow, x, at the outlet of the diffuser and μ of the two-phase ejector should meet the correlation [19]:

$$x = \frac{1}{1+\mu} \tag{11}$$

Energetic model

According to the aforementioned assumptions and the equations of conservation of mass, momentum and energy, the basic equations for the components of the TERC system can be obtained. The heat balance of the gas cooler can be expressed:

$$\dot{Q}_{gc} = \dot{m}_4(h_4 - h_5) = m_{14}(h_{15} - h_{14}) \tag{12}$$

The input powers of the LP and HP compressor:

$$W_{LP\,CM} = \dot{m}\frac{h_{2s} - h_1}{\eta_{LP\,CM}} \tag{13}$$

$$W_{HP\,CM} = \dot{m}\frac{h_{4s} - h_3}{\eta_{HP\,CM}} \tag{14}$$

The total compressor input power can be expressed:

$$W_{CM} = W_{LP\,CM} + W_{HP\,CM} \tag{15}$$

The LP and HP compressor efficiencies:

$$\eta_{LP\,CM} = 1.003 - 0.121\frac{p_2}{p_1} \tag{16}$$

$$\eta_{HP\,CM} = 1.003 - 0.121\frac{p_4}{p_3} \tag{17}$$

The refrigeration capacity of the evaporator can be represented:

$$\dot{Q}_{ev} = \dot{m}_9(h_9 - h_8) \tag{18}$$

The heat balance relationship of the intercooler can be expressed:

$$\dot{m}_6 h_6 + \dot{m}_2 h_2 = \dot{m}_3 h_3 + \dot{m}_7 h_7 \tag{19}$$

The TERC system COP can be obtained:

$$COP = \frac{Q_{ev}}{W_{CM}} \tag{20}$$

Entropy production model

Entropy can be transferred with heat and mass migration and can arise spontaneously in an irreversible process. It only increases during energy transfer and conversion, and the limiting case, *i.e.*, the entropy production in reversible processes, is zero. Entropy is a measure of the degree of irreversibility, so the entropy analysis method can clearly represent the degree of irreversibility of each component and system [20, 21]. The general expression of the entropy equation for the open system of the irreversible process:

$$\mathrm{d}S_{\mathrm{cv}} = \frac{\delta \dot{Q}}{T} + \sum \left(s_{\mathrm{i}} \delta \dot{m}_{\mathrm{i}} \right)_{\mathrm{in}} - \sum \left(s_{\mathrm{j}} \delta \dot{m}_{\mathrm{j}} \right)_{\mathrm{out}} + \delta S_{\mathrm{g}} \tag{21}$$

The entropy analysis method can clearly represent the degree of irreversibility of each component and system, and the TERC system entropy balance equation:

$$\frac{\dot{Q}_{\mathrm{gc}}}{\overline{T}_{\mathrm{gcef}}} - \frac{\dot{Q}_{\mathrm{ev}}}{\overline{T}_{\mathrm{evef}}} = \sum \delta S_{\mathrm{i}} \tag{22}$$

where $\overline{T}_{\mathrm{gcef}}$ and $\overline{T}_{\mathrm{evef}}$ denote the effective reservoir temperature of the fluid-flowing through the exterior of the gas cooler and evaporator, respectively. The temperatures and can be expressed:

$$\overline{T}_{\mathrm{gcef}} = \frac{h_{14} - h_{15}}{s_{14} - s_{15}} \tag{23}$$

$$\overline{T}_{\mathrm{evef}} = \frac{h_{16} - h_{17}}{s_{16} - s_{17}} \tag{24}$$

For the gas cooler:

$$\delta S_{\mathrm{gc}} = \dot{Q}_{\mathrm{gc}} \left(\frac{1}{\overline{T}_{\mathrm{gcef}}} - \frac{1}{\overline{T}_{\mathrm{gc}}} \right) \tag{25}$$

For HP and LP EV:

$$\delta S_{\mathrm{HP\ EV}} = \dot{m}_6 (s_6 - s_5) \tag{26}$$

$$\delta S_{\mathrm{LP\ EV}} = \dot{m}_8 (s_8 - s_7) \tag{27}$$

For HP and LP compressors:

$$\delta S_{\mathrm{HP\ CM}} = \dot{m}_4 (s_4 - s_3) \tag{28}$$

$$\delta S_{\mathrm{LP\ CM}} = \dot{m}_2 (s_2 - s_1) \tag{29}$$

For the evaporator and the ejector:

$$\delta S_{\mathrm{ev}} = \dot{Q}_{\mathrm{ev}} \left(\frac{1}{\overline{T}_{\mathrm{ev}}} - \frac{1}{\overline{T}_{\mathrm{evef}}} \right) \tag{30}$$

$$\delta S_{\mathrm{eje}} = (1 + \mu) \dot{m}_{11} s_{13} - \mu \dot{m}_{11} s_9 - \dot{m}_{11} s_3 \tag{31}$$

For the gas-liquid separator and the intercooler:

$$\delta S_{\mathrm{sep}} = (1 + \mu) \dot{m}_{11} s_{13} - \dot{m}_{11} s_1 \tag{32}$$

$$\delta \mathrm{S}_{\mathrm{inl}} = \dot{m}_3 s_3 + \dot{m}_7 s_7 - \dot{m}_6 s_6 - \dot{m}_2 s_2 \tag{33}$$

To compensate for the energy loss in the irreversible process, the additional work is:

$$\Delta W = T_0 \Delta S_{\mathrm{g}} \tag{34}$$

Results and discussion

Based on the previous models, the relevant simulation program was written in engineering equation solver, the thermodynamic properties of the refrigerant were obtained by REFPROP 9.0, the thermodynamic parameters were calculated for all state points. The performance of the TERC and CTRC systems were compared and an entropy production analysis was carried out for the TERC system. In the simulations, the operating conditions range the gas cooler outlet temperature is in the range of 30∼38 °C, the pressure p_{gc} of the gas cooler is in the range of 8∼10 MPa and the evaporation temperature is in the range of –40 °C ∼ –25 °C. In addition, the efficiencies of the ejector components are: $\eta_n = 0.85$, $\eta_s = 0.90$, $\eta_m = 0.90$, and $\eta_d = 0.85$.

Performance comparisons between TERC and CTRC system

This section investigates the effect of gas cooler outlet temperature, T_{gc}, and evaporating temperature, T_{ev}, on the CTRC system COP, TERC system COP and component entropy generation over the variation range of $T_{gc} = 30\sim38$ °C and $T_{ev} = -25$ °C ∼ –40 °C under the conditions of $p_{dis} = 9.3$ MPa and $p_{in} = 4.1$ MPa. It is observed in figs. 3(a) and 3(b) that, as the gas cooler outlet temperature decreases and evaporating temperature rises, the TERC and CTRC system COP significantly increase. Meanwhile, it can be found that the changes in COP_{TERC} and COP_{CTRC} with evaporating temperature are greater than that with gas cooler outlet temperature. Furthermore, as the evaporating temperature ranging from –40 °C to –25 °C, the LP compressor power consumption and the cooling capacity decrease, resulting in an increase in COP_{TERC} and COP_{CTRC}. In addition, the reduction in gas cooler outlet temperature brings about a decrease in HP compressor power consumption and an increase in COP_{TERC} and COP_{CTRC}. Taking the TERC system as an example, when the gas cooler outlet temperature decreases from 38-30 °C under the condition of $T_{ev} = -35$ °C, the COP increases from 0.4-0.4464 (11.6% improvement). Also, when the evaporating temperature increases from –40 °C to –25 °C under the condition of $T_{gc} = 34$ °C, the COP increases from 0.3531-0.6877 (94.8% improvement). The analysis indicates that the COP_{TERC} and COP_{CTRC} decrease by 0.0071-0.0013 and 0.0055-0.0012, respectively, for every 2 °C increase in the outlet temperature of the gas cooler and evaporating temperature. As illustrated in fig. 3(c), when the gas cooler outlet temperature increases from 30-38 °C, the δ_{COP} slowly decreases. Meanwhile, the δ_{COP} gradually declines as the evaporator temperature decreases. It can be attributed to that the COP increases with the rise of evaporating temperature, and the higher the evaporating temperature, the faster the rate of COP increase.

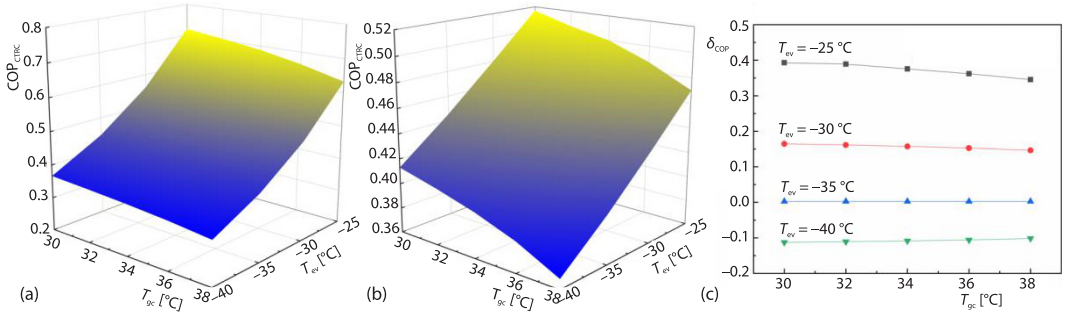

Figure 3. Effects of gas cooler outlet temperature and evaporating temperature on the TERC system COP (a) and CTRC system COP (b) as well as variation of δ_{COP} with evaporating temperature and gas cooler outlet temperature (c)

Under the same conditions, when the evaporating temperature increases, the work consumed in the compressor per unit mass of refrigerant decreases, and the COP of the system is then improved. Furthermore, COP_{TERC} increases faster than COP_{CTRC} when the gas cooler outlet temperature remains unchanged.

This part investigates the effect of intermediate pressure p_{in} and discharge pressure p_{dis} on the CTRC system COP, TERC system COP and component entropy generation over the variation range of p_{in} = 3∼5 MPa and p_{dis} = 8∼10 MPa under the conditions of p_{ev} = 1.2 MPa and T_{gc} = 35 °C. It is observed in figs. 4(a) and 4(b) that, as the discharge pressures rises, the TERC and CTRC system COP shows a trend of increasing and then decreasing. What's more, the rate of increase of COP_{TERC} and COP_{CTRC} are greater than the rate of decrease, and there is an extreme value point. This extreme point is the maximum value of COP, and its corresponding discharge pressure is the optimal discharge pressure of the system. This is mainly because: when p_{dis} is lower than the optimal discharge pressure, the increase rate of heat release per unit mass of refrigerant in the gas cooler is larger than the increase rate of compressor power consumption; when p_{dis} is higher than the optimal discharge pressure, the increase rate of heat release per unit mass of refrigerant in the gas cooler is smaller than the increase rate of compressor power consumption. At the same time, it can be found that the intermediate pressure also affects COP_{TERC} and COP_{CTRC} to some extent. Taking the TERC system as an example, when the discharge pressure increases from 8-10 MPa under the condition of p_{in} = 4 MPa, the range of variation of the maximum COP is 0.3745-0.4378. Also, when the intermediate pressure increases from 3-5 MPa under the condition of p_{dis} = 9.0 MPa, the range of variation of the maximum COP is 0.3531-0.5721. As illustrated in fig. 4(c), when the intermediate and pressures increases from 3-5 MPa, the δ_{COP} shows a clear downward trend. At the same time, the δ_{COP} gradually raises as the discharge pressure increases.

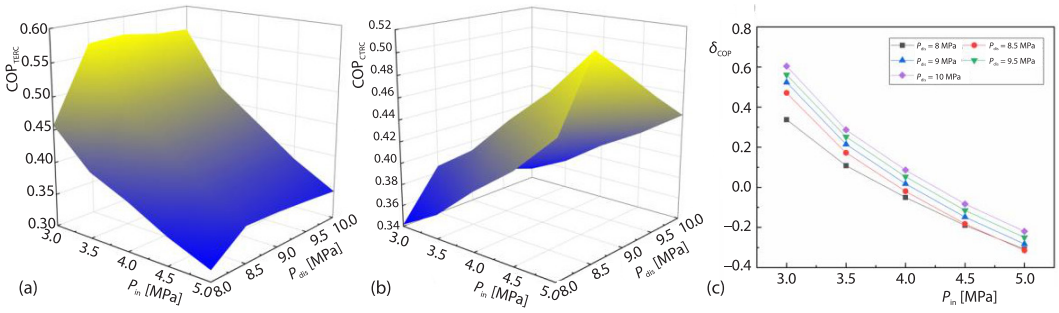

Figure 4. Effects of intermediate and discharge pressures on the TERC system COP (a) and CTRC system COP (b) as well as variation of δ_{COP} with intermediate and discharge pressures (c)

This section investigates the effect of intermediate pressure, p_{in}, and evaporating temperature, T_{ev}, on the CTRC system COP, TERC system COP and component entropy generation over the variation range of p_{in} = 3∼5 MPa and T_{ev} = –25 °C ∼ –40 °C under the conditions of p_{dis} = 9.3 MPa and T_{gc} = 35 °C. It is observed in figs. 5(a) and 5(b) that, as the intermediate pressure decreases and evaporating temperature rises, the TERC and CTRC system COP significantly increase. Furthermore, as the evaporating temperature ranging from –40 °C to –25 °C, the LP compressor power consumption and the cooling capacity decrease, resulting in an increase in COP_{TERC} and COP_{CTRC}. In addition, the increase of the intermediate pressure brings about a decrease in COP_{TERC} and COP_{CTRC}. Although the power consumption of the LP compressor increases and the HP compressor power consumption decreases, the total power

consumption of the compressor is increased. At the same time, we can find that the TERC system COP varies more with the intermediate pressure compared to the CTRC system COP. Taking the TERC system as an example, when the evaporating temperature increases from –40 °C to –25 °C under the condition of p_{in} = 4 MPa, the COP increases from 0.3649-0.7167 (96.4% improvement). Also, when the intermediate pressure decreases from 5-3 MPa under the condition of T_{ev} = –35 °C, the COP increases from 0.2912-0.7619 (161.6% improvement). As demonstrated in fig. 5(c), when the intermediate pressure increases from 3-5 MPa, the δ_{COP} has a significant decreasing trend. The evaporating temperature decreases, the degree of decline of the curve tends to level off. At the same time, as the evaporating temperature decreases, δ_{COP} shows a decreasing trend.

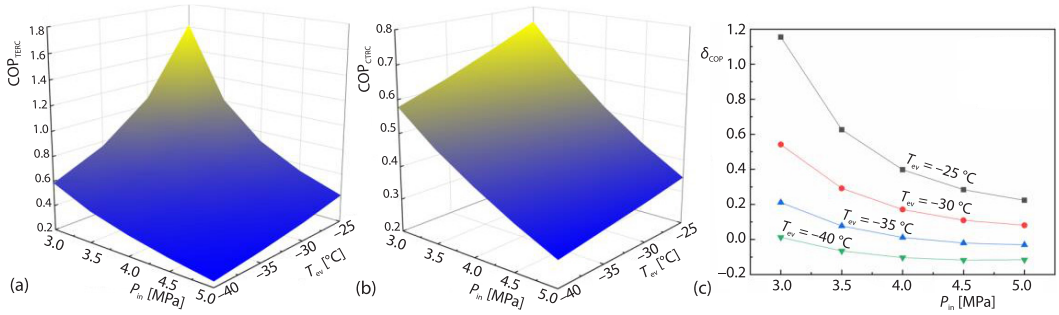

Figure 5. Effects of intermediate pressure and evaporating temperature on the TERC system COP (a) and CTRC system COP (b) as well as variation of δ_{COP} with intermediate pressure and evaporating temperature (c)

Entropy analysis of TERC system

Table 1 lists the thermodynamic data of the working fluid when the TERC system is operated under real conditions. Based on the aforementioned actual working conditions, this work focuses on the analysis of the cycle components and the power capacity loss of each process. The entropy analysis method was used to obtain the distribution of the power capability loss of the whole cycle process and components as illustrated in fig. 6. It can be noticed that the power capability loss of the ejector is the largest, accounting for 26.95% of the power capability loss of the whole system. This was followed by the LP compressor, which accounted for 26.06%. After these two-components, the other components contribute in the following order: HP EV, HP compressor, intercooler, LP EV, evaporator and gas cooler. In addition, we can find that the total power capability loss for all components of the TERC system is 20.87 kW. Under the same working conditions, the total power capability loss for all components of the CTRC system is 28.16 kW. We know that the greater the power capability loss of a system, the greater the degree to which thermodynamically irreversible processes are taking place, and the lower the energy grade and availability.

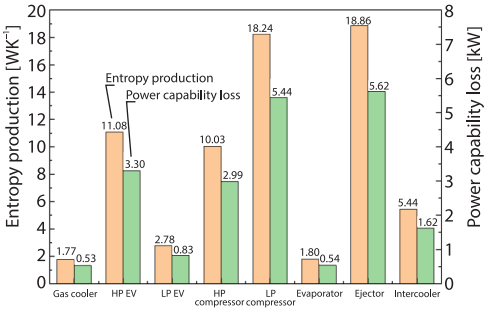

Figure 6. Schematic diagram of entropy production and distribution of power capability loss among all components for the TERC system

Table 1. Thermodynamic properties of the TERC system at different state points under real conditions

Location	Fluid	$\dot{m}$ [kgs^{-1}]	T [°C]	p [MPa]	h [kJkg^{-1}]	s [kJkg^{-1}K^{-1}]
1	CO_2	0.447	–22.886	1.8	437.04	1.9628
2	CO_2	0.447	44.254	4.1	484.22	2.0036
3	CO_2	0.684	6.2695	4.1	426.44	1.8086
4	CO_2	0.302	74.569	9.3	468.77	1.8418
5	CO_2	0.302	35	9.3	295.43	1.3030
6	CO_2	0.302	6.2695	4.1	295.43	1.3397
7	CO_2	0.065	6.2695	4.1	215.78	1.0547
8	CO_2	0.065	–35.057	1.2	215.78	1.0974
9	CO_2	0.065	–35.057	1.2	436.22	2.0233
10	CO_2	0.065	–44.135	0.86	424.89	2.0288
11	CO_2	0.382	–44.135	0.86	382.26	1.8427
12	CO_2	0.447	–44.135	0.86	387.26	1.8645
13	CO_2	0.447	–22.886	1.8	416.83	1.8820
14	Water	0.530	26	0.101325	109.10	0.38120
15	Water	0.530	65	0.101325	272.18	0.89361
16	Air	2.849	–25	0.101325	248.15	6.6757
17	Air	2.849	–30	0.101325	243.12	6.6552
0	Air	–	25	0.101325	298.45	6.8603

The fact that the maximum power capacity loss occurs in the ejector suggests that more attention should be given to the design of the ejector to reduce irreversible losses, which can significantly improve system performance. The generation of irreversible losses in the ejector can be attributed to the following. Firstly, as the primary flow passes through the working nozzle, it undergoes a non-ideal adiabatic process due to friction and incurs irreversible losses. Secondly, the entrainment ratio of the ejector can have a large impact on system losses. If the entrainment ratio is low, it will result in higher working fluid-flow, as well as increase the fluid and ejector friction, thus causing a larger power capacity loss. Therefore, the proper design of the ejector is the key to reduction of system losses. In addition, the power capacity loss of the gas cooler, evaporator and intercooler are all caused by unequal heat transfer. Further improving the heat transfer performance of these components can effectively reduce the power capacity loss of the whole TERC system.

Figure 7(a) exhibits the effect on the entropy production of each component in the TERC system by the gas cooler outlet temperature under the conditions of T_{ev} = –35 °C, p_{dis} = 9.3 MPa and p_{in} = 4.1 MPa. From fig. 7(a), it can be observed that the entropy production of the HP EV and HP compressor increases as the gas cooler outlet temperature raises. This is because the throttling pressure drop of the high pressure supercritical CO_2 fluid occurs in the HP EV, and the friction loss of this process increases sharply as the temperature of the supercritical CO_2 fluid increases. The increase in the outlet temperature of the gas cooler increases the flow of CO_2 fluid through the HP compressor, leading to an increase in its entropy production. In addition, the entropy production of the gas cooler decreases slightly. Apart from the HP EV, HP compressor and gas cooler, the entropy production of other components is basically unchanged.

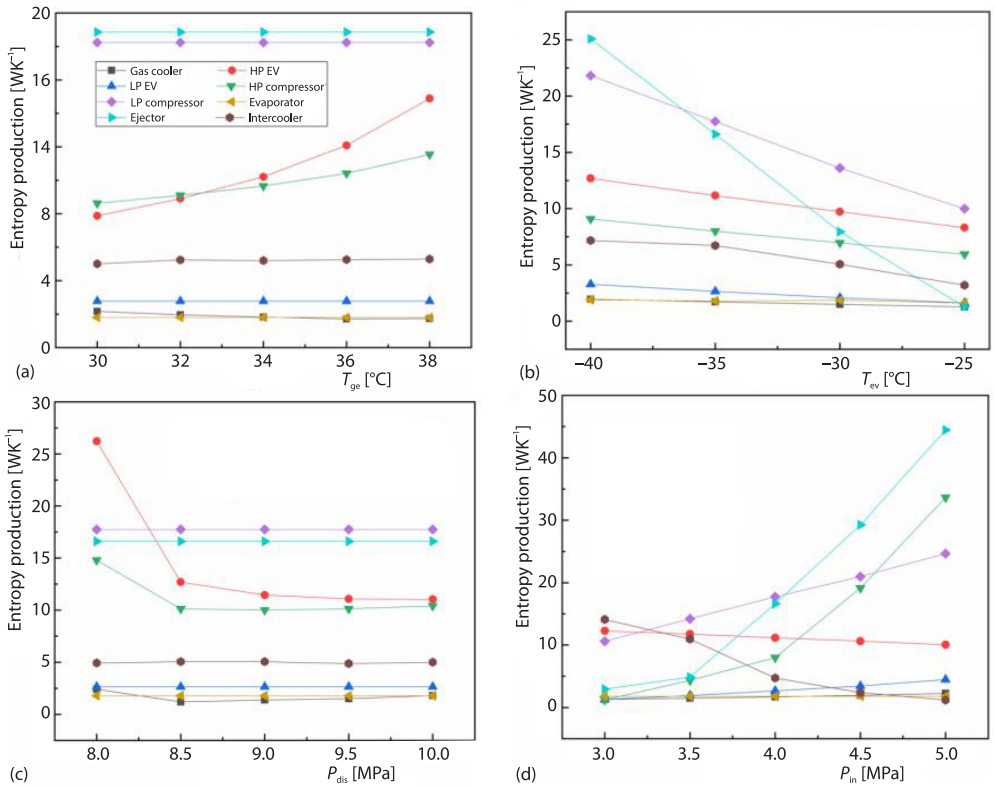

Figure 7. Effect on the entropy production of each component in the TERC system by the gas cooler outlet temperature (a), evaporating temperature (b), discharge pressure (c), and intermediate pressure (d)

Figure 7(b) demonstrates the effect on the entropy production of each component in the TERC system by the evaporating temperature under the conditions of T_{gc} = 35 °C, p_{dis} = 9.3 MPa, and p_{in} = 4.1 MPa. As can be seen from fig.7(b), with the increase of the evaporating temperature, the entropy production of the main components of the system are reduced to different degrees. The most obvious trend is the decrease of the entropy production of the ejector, while the total entropy production of the system is also reduced. This is because the increase of the evaporating temperature, the entrainment ratio and the performance coefficient and mechanical performance coefficient of the system are increased, and the temperature difference with the room temperature is reduced, and the irreversible loss caused by the system isothermal heat transfer is reduced. Meanwhile, fig. 7(c) exbibits the effect on the entropy production of each component in the TERC system by the discharge pressure under the conditions of p_{ev} = 1.2 MPa, p_{dis} = 9.3 MPa, and p_{in} = 4.1 MPa. As can be seen from fig. 7(c), with the increase of discharge pressure, the entropy production of the HP EV decreases. This can be attributed to the decrease in flow through HP EV. When the discharge pressure is higher than 8.5 MPa, the entropy production of the gas cooler and HP compressor rise slowly with the increase of discharge pressure. Obviously, the rise in discharge pressure increases the compressor power consumption and irreversible losses. Furthermore, the discharge pressure has basically no effect on the entropy production of the LP compressor, ejector, intercooler, LP EV and evaporator. Figure 7(d) reveals the effect on the entropy production of each component in the TERC system by the intermediate

pressure under the conditions of p_{ev} = 1.2 MPa, p_{dis} = 9.3 MPa, and T_{gc} = 35 °C. It can be seen that as the intermediate pressure raises, the entropy production of the ejector, HP compressor, LP compressor, LP EV and gas cooler increases. The main cause of entropy production in two-stage ejector is the non-ideal adiabatic expansion of the working fluid as it passes through the working nozzle of the ejector, as well as the frictional collision of the working fluid when the primary and secondary fluids mix with each other in the supersonic flow regime.

Conclusions

The thermodynamic performance of this two-stage compression/ejector refrigeration system is analyzed in terms of energy and entropy, and the influence of the main operating parameters such as gas cooler outlet temperature, exhaust pressure, intermediate pressure and evaporation temperature on the system performance is discussed in detail and compared with a CTRC system under the same operating conditions. Concluding remarks are as follows.

- As the gas cooler outlet temperature decreases and evaporating temperature rises, the TERC and CTRC system COP significantly increase. Meanwhile, the analysis indicates that the COPTERC and COPCTRC decrease by 0.0071-0.0013 and 0.0055-0.0012, respectively, for every 2 °C increase in the outlet temperature of the gas cooler and evaporating temperature.
- In terms of TERC system, when the discharge pressure increases from 8-10 MPa under the condition of p_{in} = 4 MPa, the range of variation of the maximum COP is 0.3745-0.4378. Also, when the intermediate pressure increases from 3-5 MPa under the condition of p_{dis} = 9.0 MPa, the range of variation of the maximum COP is 0.3531-0.5721.
- The entropy analysis of the TERC system shows that the ejector has the largest entropy production, accounting for 26.95% of the whole system, followed by the low pressure compressor with 26.06%. The system can be adjusted to the changing operating conditions using two or more stage ejectors to maintain optimum system performance.
- In addition, the performance of the ejector does not depend on the outlet temperature of the gas cooler or the discharge pressure of the high pressure stage. However, it decreases significantly with increasing evaporating temperature and increases significantly with increasing intermediate pressure.

Acknowledgment

This paper is supported by China Agriculture Research System of MOF and MARA (CARS-47) and Shanghai Professional Technology Service Platform on Cold Chain Equipment Performance and Energy Saving Testing Evaluation (20DZ2292200).

Contribute

Dazhang Yang and Yang Li contributed equally to this study.

Nomenclature

h – specific enthalpy, [kJ/kg]
$\dot{m}$ – mass-flow rate, [kg/s]
p – pressure, [MPa]
$\dot{Q}_{ev}$ – refrigeration capacity of the evaporator, [kW]
$\dot{Q}_{gc}$ – heat release of the gas cooler, [kW]
S – entropy, [kJ/K]
s – specific entropy [kJkg^{-1}K^{-1}]
$\overline{T}$ – effective reservoir temperature, [°C]
T – temperature, [°C]
u – velocity, [m/s]
W – compressor input power, [kW]
x – quality of the flow

Greek symbols

η – efficiency
μ – entrainment ratio

Subscripts

CM – compressor
cv – control volume

d – diffuser
dis – discharge
ev – evaporator
eje – ejector
evef – fluid at the exterior of the evaporator
g – gas
gc – gas cooler
gcef – fluid at the exterior of the gas cooler
HP – high pressure
i,j – location
in – inlet/intermediate
inl – intercooler
is – isentropic process
k – component
LP – low pressure
m – mixing chamber
n – working nozzle
out – outlet
s – suction chamber
sep – gas-liquid separator
sys – system
1-17 – state point
0 – reference condition

References

[1] Yilmaz, O., *et al*., Experimental Energy and Exergy Analyses of Ship Refrigeration System Operated by Frequency Inverter at Varying Sea Water Temperatures, *Journal of the Brazilian Society of Mechanical Sciences and Engineering*, *44* (2022), 4, pp. 1-23
[2] Ezgi, C., Design and Thermodynamic Analysis of Waste Heat-Driven Zeolite-Water Continuous-Adsorption Refrigeration and Heat Pump System for Ships, *Energies*, *14* (2021), 3, 699
[3] Yang, D., *et al.*, Research and Application Progress of Transcritical CO_2 Refrigeration Cycle Cystem: A review, *International Journal of Low-Carbon Technologies*, *17* (2021), Dec., pp. 245-256
[4] Jia, F., *et al*., Numerical Investigation on the Performance of Two-Throat Nozzle Ejectors with Different Mixing Chamber Structural Parameters, *Energies*, *14* (2021), 6900
[5] Liang, Y., *et al*., Investigation of a Refrigeration System Based on Combined Supercritical CO_2 Power and Transcritical CO_2 Refrigeration Cycles by Waste Heat Recovery of Engine, *International Journal of Refrigeration*, *118* (2020), Oct., pp. 70-482
[6] Morosuk, T., *et al*., Entropy-Cycle Method for Analysis of Refrigeration Machine and Heat Pump Cycles, *Thermal Science*, *10* (2006), 1, pp. 111-124
[7] Foroozesh, F., *et al.*, Improvement of the Wet Steam Ejector Performance in a Refrigeration Cycle Via Changing the Ejector Geometry by a Novel EEC (Entropy Generation, Entrainment Ratio, and Coefficient of Performance) Method, *International Journal of Refrigeration*, *110* (2020), Feb., pp. 248-261
[8] Ji, Y., *et al*., A Thermodynamic Entropy Analysis of Solar-Driven Ejector Refrigeration Circulation, *Cryogenics and Superconductivity*, *36* (2008), 12, 5
[9] Ramirez-Minguela, J. J., *et al*., Entropy Generation Analysis of a Solid Oxide Fuel Cell by Computational Fluid Dynamics: Influence of Electrochemical Model and Its Parameters, *Thermal Science*, *22* (2018), 1B, pp. 577-589
[10] Volodymyr, I., *et al*., Hybrid Two-Stage CO_2 Transcritical Mechanical Compression-Ejector Cooling Cycle: Thermodynamic Analysis and Optimization, *International Journal of Refrigeration*, *132* (2021), Dec., pp. 45-55
[11] Zeng, M., *et al.*, Thermodynamic Analysis of the Effect of Internal Heat Exchanger on the Dual-Ejector Transcritical CO_2 Cycle for Low-Temperature Refrigeration, *International Journal of Energy Research*, *46* (2022), 9, pp. 12702-12721
[12] Liu, Y., *et al*., Theoretical Analysis on a Novel Two-Stage Compression Transcritical CO_2 Dual-Evaporator Refrigeration Cycle with an Ejector, *International Journal of Refrigeration*, *119* (2020), Nov., pp. 268-275
[13] Yang, D., *et al.*, Exergy Destruction Characteristics of a Transcritical Carbon Dioxide Two-Stage Compression/Ejector Refrigeration System for Low-Temperature Cold Storage, *Energy Reports*, *8* (2022), Nov., pp. 8546-8562
[14] Manjili, F. E., Yavari, M. A., Performance of a New Two-Stage Multi-Intercooling Transcritical CO_2 Ejector Refrigeration Cycle, *Applied Thermal Engineering*, *40* (2012), July, pp. 202-209
[15] J. Chen, *et al*., Evaluation of the Ejector Refrigeration System with Environmentally Friendly Working Fluids from Energy, Conventional Exergy and Advanced Exergy Perspectives, *Energy Conversion and Management*, *148* (2017), Sept., pp. 1208-1224
[16] Yuan, H., *et al.*, Performance Analysis of a Solar-Assisted OTEC Cycle for Power Generation and Fishery Cold Storage Refrigeration, *Applied Thermal Engineering*, *90* (2015), Nov., pp. 809-819
[17] Cao, X., *et al.*, Performance Analysis of an Ejector-Assisted Two-Stage Evaporation Single-Stage Vapor-Compression Cycle, *Applied Thermal Engineering*, *205* (2022), 118005

[18] Morosuk, T., *et al*., Conventional Thermodynamic and Advanced Exergetic Analysis of a Refrigeration Machine Using a Voorhees' Compression Process, *Energy Conversion and Management*, *60* (2012), Aug., pp. 143-151
[19] Bai, T., *et al*., Thermodynamic Analyses on an Ejector Enhanced CO_2 Transcritical Heat Pump Cycle with Vapor-Injection, *International Journal of Refrigeration*, *58* (2015), Oct., pp. 22-34
[20] Hristov, J., *et al.*, Research Note on a Parabolic Heat-Balance Integral Method with Unspecified Exponent: An Entropy Generation Approach in Optimal Profile Determination, *Thermal Science*, *13* (2009), 2, pp. 49-59
[21] Aikkalp, E., Models for Optimum Thermo-Ecological Criteria of Actual Thermal Cycles, *Thermal Science*, *17* (2012), 3, pp. 915-930

Paper submitted: July 2, 2022
Paper revised: September 22, 2022
Paper accepted: September 29, 2022